CHAPTER-6

SENSITIVENESS OF AXIAL MAGNETIC FIELD ON ELECTRON ACCELERATION BY A RADIALLY POLARIZED LASER PULSE IN VACUUM

6.1 INTRODUCTION

Laser particle interaction is an advancing area of research to explore the electron energy gains. Many theoretical and experimental models were proposed and developed which target the sequential improvement in electron energy gains [13, 35, 60, 105]. Wang *et al.* [105] reported laser plasma acceleration to $2GeV$ with pettawatt pulses. The characteristics variations of laser parameters such as pulse polarizations, beam width, initial phase and frequency amplifications plays important role in improvements of electron energy gain. The ultra-short high power laser based on chirped-pulse amplification technique was explored [35, 96]. Sohbatzadeh and Aku [96] have investigated the role of polarization with chirped Gaussian laser pulse for electron bunch acceleration with linear, elliptical and circular polarization in vacuum. For a tightly focused RP laser pulse, the longitudinal component of electric field plays a vital role in the electron acceleration [36]. The external magnetic field enhances $\vec{v}\times\vec{B}$ force due to which the electron moves around the direction of propagation of the laser pulse efficiently. The magnetic field also increases the electron energy gain during laser induced acceleration [55]. Additional acceleration by magnetic field resonance [58] at very high intensity laser interaction was proposed with spontaneous magnetic field of $100MG$. RP laser beams were explored because of their inherent complete symmetry which leads to high trapping and acceleration of electrons [66, 86, 97, 102]. The electron gain and retain high energy till the saturation of betatron resonance. Lu *et al.* [102] studied the electron acceleration by a tightly focused RP laser pulse in vacuum. They presented a non-paraxial solution for a RP laser pulse in accordance with a plane wave angular spectrum analysis (ASA) of electromagnetic field structure. They compared the results with paraxial approximation (PA) solution and reported a larger energy gain by electron with a non-paraxial solution even if the beam waist size is much larger than laser wavelength. Singh [64] studied the acceleration of electrons by a circularly polarized laser pulse with an intense axial magnetic field in vacuum and calculated the energy gain of the order of GeV with low emittance. The combined effect of polarization and external magnetic field further improves the electron trajectories with enhanced energy gain [64, 121, 122]. Sajal and Tripathi [75] studied the effect of azimuthal magnetic field on electron acceleration by varying the magnetic field parameter upto $40MG$. They observed that electron undergoes betatron oscillation under the influence of magnetic field, which increases the duration time of interaction of electron with laser pulse, resulting in more energy gain by the electrons. Bochkareva *et al.* [67] investigated electron acceleration by RP, ultra-short, relativistic strong laser pulse. They proposed that the electrons are accelerated by laser field and are subject to condition that the focal spot diameter is of the order of laser wavelength. This occurs when laser light interacts with nano-objects. They presented that the field phase averaged energy is maximum under moderately tight focusing than extremely tight focusing due to optimal phase of laser field. Varin *et al.* [106] presented broad overviews of longitudinal electron acceleration by a tightly focused laser pulse. They confirmed the direct acceleration of electron at rest by longitudinal electric field component can be done experimentally with a high power infrared laser source at the advanced laser light source (ALLS) facility. However, the limitation appeared as a low conversion efficiency of fundamental Gaussian mode to RP mode.

In this chapter we have presented a RP laser pulse for electron acceleration with an intense magnetic field in vacuum. An electron while interacting with RP laser pulse experiences a force due to longitudinal component of electric field of laser. As a result electron is accelerated around the direction of propagation of the laser with high energy gain. The energy gain can further be increased by using higher intensity laser pulse. Hence, the rest electron is accelerated to high energy by using a RP laser pulse in vacuum. The accelerated electron after attaining the high relativistic energy tends to go out of phase with laser field which leads to deceleration and lost its gained energy. The presence of axial magnetic field improves the strength of $\vec{v} \times \vec{B}$ force which supports the retaining of betatron resonance for longer duration. Hence, restrict deceleration of electron and support in retaining of gained energy for longer duration. The experimental availability of magnetic field of the order of MG [113, 115] favours our model to use axial magnetic field for electron acceleration with a RP laser pulse in vacuum. This paper is organized as follows. Section 6.2 and 6.3, describes the electromagnetic fields and electron dynamics used to study the electron acceleration. Results and discussion are described in section 6.4. Finally, conclusions are drawn in the section 6.5.

6.2 FIELD DISTRIBUTION FOR RADIALLY POLARIZED LASER PULSE

A RP laser beam propagating parallel to the z-axis with electric field ($\vec{E} = \hat{r}E_r + \hat{z}E_z$) component is expressed as [97]:

$$E_r = E_0 \frac{r}{r_0 f^2}\cos(\phi)\exp\left[-\left\{\frac{[t-(z-z_L)/c]^2}{\tau^2}\right\}-\frac{r^2}{r_0^2 f^2}\right], \tag{6.1}$$

$$E_z = E_0 \frac{2}{k_0 r_0 f^2}\left[\left(1-\frac{r^2}{r_0^2 f^2}\right)\sin(\phi)-\frac{zr^2}{Z_R r_0^2 f^2}\cos(\phi)\right]\exp\left[-\left\{\frac{[t-(z-z_L)/c]^2}{\tau^2}\right\}-\frac{r^2}{r_0^2 f^2}\right], \tag{6.2}$$

where $\phi = \omega_0 t - k_0 z + 2\tan^{-1}(z/Z_R) - zr^2/(Z_R r_0^2 f^2) + \phi_0$, $f^2 = 1 + (z/Z_R)^2$, $k_0 = \omega_0 / c$, $Z_R = k_0 r_0^2 / 2$ is the Rayleigh length, r is the radial coordinate, τ is the pulse duration, r_0 is minimum laser spot size, ω_0 is the laser frequency, z_L is the initial position of pulse peak and c is the velocity of light in vacuum. Equations (6.1) and (6.2) represent a simple paraxial approximation solution of a RP laser pulse. These equations are not valid for a tightly focused laser pulse in its present form. Electron acceleration with a tightly focused RP laser pulse depends on a non paraxial approach for its accurate description [67, 102, 106].

The magnetic field components related to the laser pulse can derive through Maxwell's equation $\vec{\nabla} \times \vec{E}_L = -\partial \vec{B}_L / \partial t$ and expressed as:

$$B_{Lr} = 0,\ B_{L\theta} = E_r / c,\ B_{Lz} = 0, \tag{6.3}$$

The externally applied short duration intense axial magnetic field [64] is given by:

$$\vec{B}_S = \hat{z}B_0 \exp\left(-\frac{t^2}{\tau_b^2}\right), \tag{6.4}$$

where τ_b is the duration of magnetic field. The total magnetic field is $\vec{B} = \vec{B}_L + \vec{B}_S$.

Figure 6.1 shows a scheme of electron acceleration by a RP laser pulse with axial magnetic field in vacuum.

6.3 ELECTRON DYNAMICS AND RELATIVISTICS ANALYSIS

The equations governing electron momentum and energy are the following:

$$\frac{dp_r}{dt} = -eE_r + e\beta_z B_{L\theta}, \tag{6.5}$$

$$\frac{dp_\theta}{dt} = -e\beta_r B_{Sz}, \tag{6.6}$$

$$\frac{dp_z}{dt} = -eE_z + e\beta_r B_{L\theta}, \tag{6.7}$$

$$\frac{d\gamma}{dt} = -e(\beta_r E_r + \beta_z E_z), \tag{6.8}$$

where $\gamma^2 = 1 + (p_r^2 + p_z^2)/m_0^2c^2$ is the Lorentz factor, p_r, p_θ, and p_z are the components of electron momentum $\vec{p} = \gamma m_0 \vec{v}$ respectively, β_r and β_z are the radial and longitudinal components of the normalized velocity $\vec{\beta} = \vec{v}/c$ respectively, $-e$ and m_0 are the electron's charge and rest mass respectively.

The equations (6.5)-(6.8) form a set of coupled ordinary differential equations. These equations have been solved numerically with a computer simulation code for electron trajectory and energy. Throughout this paper, time, length, velocity, momentum, and energy are normalized by $1/\omega_0$, c/ω_0, c, m_0c, and m_0c^2 respectively. The normalized laser intensity and normalized magnetic field parameter can be expressed as, $a_0 = eE_0/m_0\omega_0 c$ and $b_0 = eB_0/m_0\omega_0 c$ respectively.

6.4 RESULTS AND DISCUSSION

In all simulation below we set normalized parameters, $a_0 = 25$ (corresponding to laser intensity $I \sim 8.5\times10^{20}\ W/cm^2$), $a_0 = 100$ (corresponding to laser intensity $I \sim 1.36\times10^{22}\ W/cm^2$) and wave length $\lambda_0 \sim 1\mu m$; $b_0 = 0.0004$(corresponding to magnetic field $\sim 43kG$), $b_0 = 0.03$(corresponding to magnetic field $\sim 3MG$); laser spot sizes $r_0 = a_0$ and $a_0/2$ (corresponding values of laser spot size are $16\mu m$ and $8\mu m$ with $a_0 = 100$); laser pulse duration $\tau = 200$; initial position of pulse peak $z_L = 0$; initial electron position $z_0 = 0$ and $r_i = r_0/2$, $r_0/5$; initial phase $\phi_0 = \pi$ and magnetic field duration $\tau_b = 10^9$. We have treated $z_0 = 0$ as the best focus case. It is because according to equation (6.1), with $z_0 = 0$, the longitudinal component of electric field of the laser pulse becomes proportional to $\sin(\phi)$ and the electric force on electrons becomes positive in the z-direction [97]. This makes the initial phase $\phi = \pi$ as an accelerating phase at which the electron gains maximum energy with least scattering. Yanovsky *et al.* [77] experimentally demonstrated the availability of laser intensity of the order of $10^{22}\ W/cm^2$ with wavelength $1\mu m$ and laser spot size of few microns.

Figure 6.2 shows the variation of electron energy gain with normalized magnetic field b_0. The energy gain is analysed for distinct values of intensity parameter $a_0 = 25$, 50, 75, and 100 at $r_0 = a_0/2$ and $r_i = r_0/2$. The higher energy gain appears with axial magnetic field. The electron energy gain appears sensitive to the axial magnetic field. For $a_0 = 25$ and 100 the optimum values of b_0 for higher energy gain are 0.002 and 0.0004 respectively. Thus for high energy gain the optimum values of axial magnetic field remains small even for high intensity laser pulse. One may notice that even for small change in axial magnetic field, a significant change in electron energy appears.

Figure 6.3 shows the variation plot of electron energy gain with initial phase ϕ_0. The energy gain is analysed for distinct values of normalized intensity parameter $a_0 = 25$, 50, 75, and 100 at $r_0 = a_0/2$ and $r_i = r_0/2$ and the respective optimum values of applied magnetic field b_0 as obtained from fig. 6.2. The higher energy gain appears with axial magnetic field at initial phase $\phi_0 = \pi$ of laser pulse.

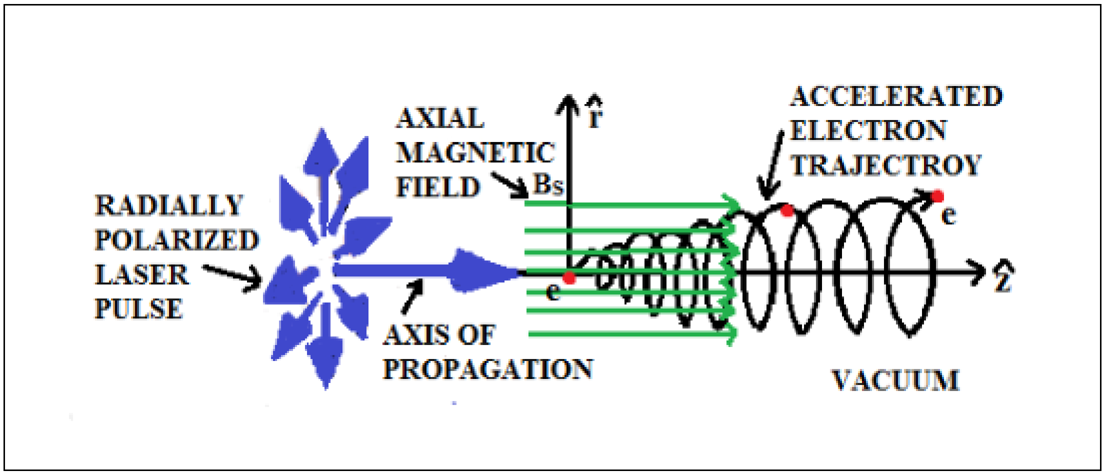

Figure 6.1. A schematic for vacuum acceleration of electron by a Radially polarized (RP) laser pulse with axial magnetic field.

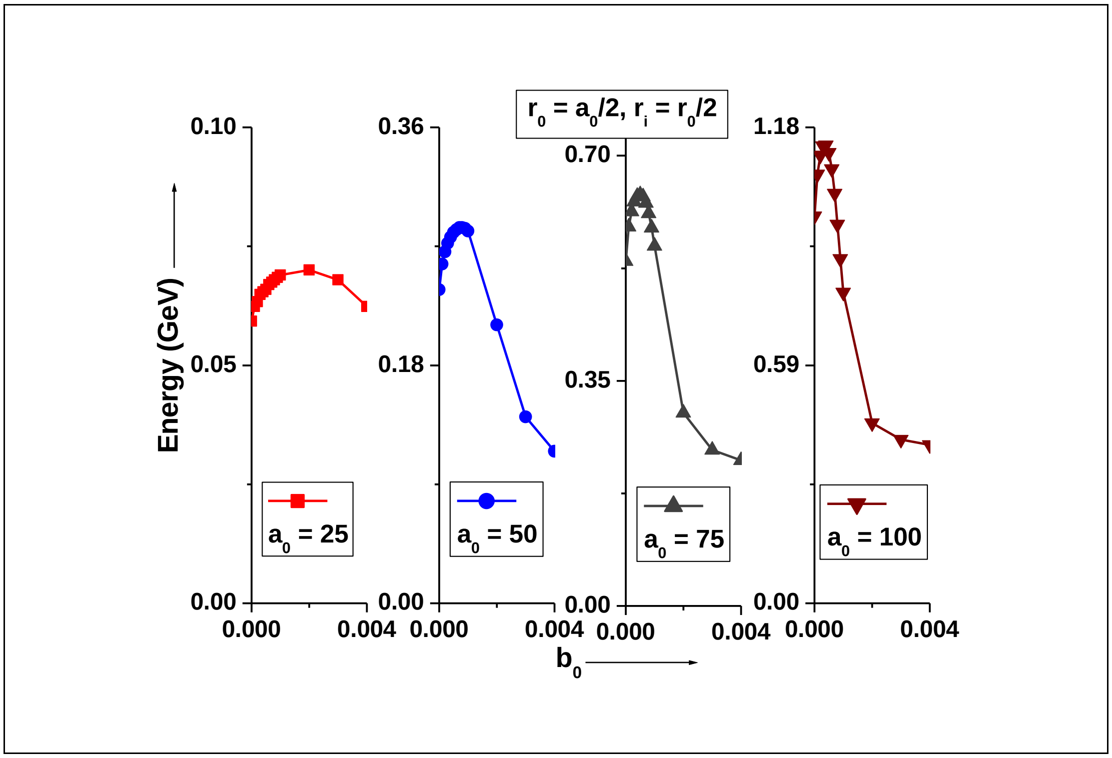

Figure 6.2. Electron energy gain as a function of normalized magnetic field b_0 **with** $r_0 = a_0/2$ **and** $r_i = r_0/2$ **for laser intensity parameter** $a_0 = 25, \ 50, \ 75,$ **and** 100 **. The other parameters are** $\tau = 200$**,** $z_L = 0$**,** $z_0 = 0$**,** $\phi_0 = \pi$**, and** $\tau_b = 10^9$**.**

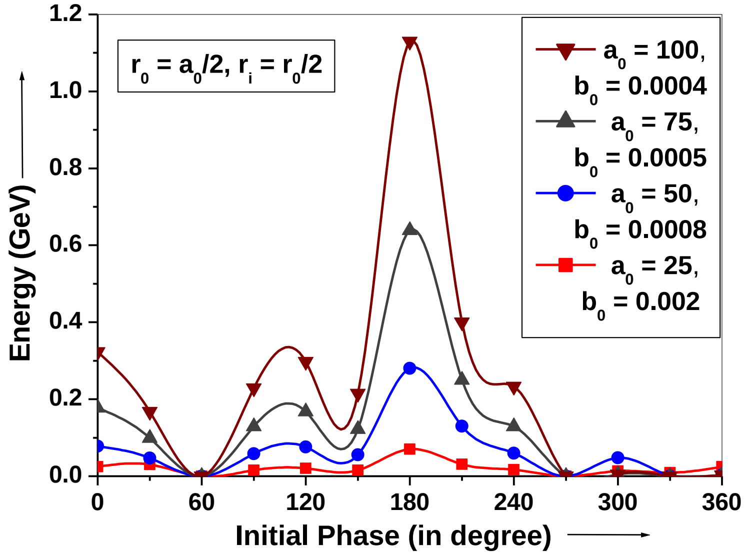

Figure 6.3. Electron energy gain variation with initial phase ϕ_0 for $r_0 = a_0/2$ and $r_i = r_0/2$ at laser intensity parameter $a_0 = 25, 50, 75,$ and 100 with respective values of normalized magnetic field as obtained from fig 6.2. The other parameters are $\tau = 200$, $z_L = 0$, $z_0 = 0$, and $\tau_b = 10^9$.

Figure 6.4 shows the electron trajectories in $r - z$ plane at $r_i = r_0/2$ for $r_0 = a_0/2$ and $r_0 = a_0$ with different values of laser intensity parameter $a_0 = 25$, 50, 75 and 100 in the absence and presence of axial magnetic field. The scattering of electron in the presence of axial magnetic field is relatively smaller than that in the absence of axial magnetic field. As appearing in fig. 6.4(a), the scattering in the presence of axial magnetic field is significantly reduced for $a_0 = 25$ whereas such reduction is apparently small for higher intensities ($a_0 = 75$ and 100). The scattering further decreases with increase in the laser spot size as depicted in fig. 6.4(b). The axial magnetic field features with the collimation of small particles. It supports in controlling the electrons going out of phase after saturation of betatron resonance. Hence keep the electron motion close to

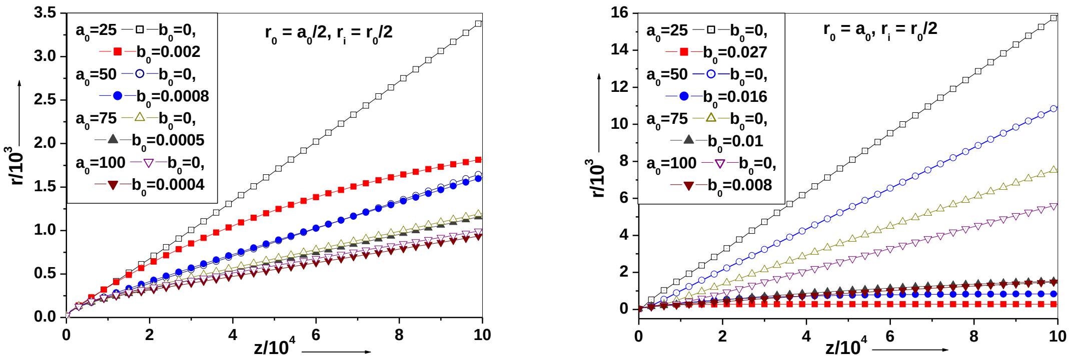

(a) **(b)**

Figure 6.4. Trajectory of electron in the $r-z$ plane without and with magnetic field for $r_i = r_0/2$ at laser intensity parameters $a_0 = 25,\ 50,\ 75,$ and 100. (a) $r_0 = a_0/2$ and (b) $r_0 = a_0$. The other parameters are $\tau = 200$, $z_L = 0$, $z_0 = 0$, $\phi_0 = \pi$, and $\tau_b = 10^9$.

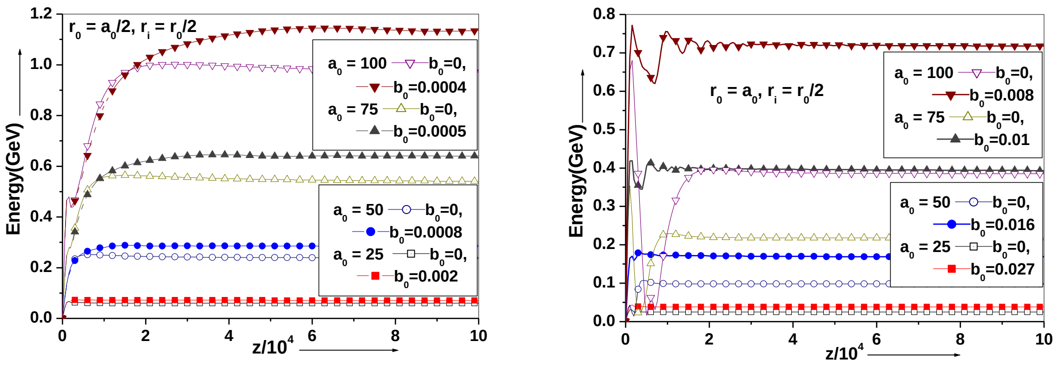

(a) **(b)**

Figure 6.5. Electron energy gain with normalized distance in the absence and presence of a applied magnetic field with $r_i = r_0/2$ for laser intensity parameters $a_0 = 25,\ 50,\ 75,$ and 100. (a) $r_0 = a_0/2$ and (b) $r_0 = a_0$. The other parameters are same as taken in fig. 6.4.

the axis of propagation of laser pulse. Thus a reduced scattering is appeared with applied magnetic field.

Figure 6.5 shows the electron energy gain with normalized distance for $r_i = r_0 / 2$ with $r_0 = a_0 / 2$ and $r_0 = a_0$ at different values of laser intensity parameter $a_0 = 25$, 50, 75 and 100 . The net energy gain by the electrons during their acceleration is sensitive to the laser spot size, laser intensity and the axial magnetic field. It is observed that the electron gains relatively higher energy with axial magnetic field for same set of parameters as in the absence of axial magnetic field. It is because of axial magnetic field which increases the duration of interaction between the laser pulse and the electron. Hence electron gains much energy from the laser field and it is accelerated. Thus the retainable energy of the accelerated electrons is also increased in this case. The electron gains nearly $1.135 GeV$ for $r_0 = a_0 / 2$ and nearly $0.72 GeV$ energy for $r_0 = a_0$ with $a_0 = 100$, in the presence of axial magnetic field with normalized magnetic field, $b_0 = 0.0004$ (corresponding to magnetic field $\sim 43 kG$) and $b_0 = 0.008$ (corresponding to $\sim 0.85 MG$) respectively. The attained energy values for $r_0 = a_0$ with $a_0 = 25$, 50, 75 and 100 are about 70% higher than the energy values obtained in the absence of magnetic field. The magnetic field parameter b_0 is optimized for maximum energy gain with respect to laser intensity and minimum spot size. We have applied axial magnetic field of the order of MG. Such magnetic field is feasibly available [113, 115] experimentally.

In figures 6.6 and 6.7, we have plotted the electron trajectory and the electron energy gain as a function of normalized distance at $r_i = r_0 / 5$ for $r_0 = a_0$ with different values of laser intensity parameter $a_0 = 25$, 50, 75 and 100 . We have observed a relatively higher energy gain in the presence of axial magnetic field with $r_i = r_0 / 5$ for $r_0 = a_0$ than that with $r_i = 0$ for $r_0 = a_0$ in the absence of axial magnetic field. As reported in Ref. 97, the electron gains $2.7 GeV$ of energy for $r_0 = 100$, $r_i = 0$ with $a_0 = 100$. However, we obtain $5.2 GeV$ energy for $r_0 = 100$, $r_i = r_0 / 5$ with $a_0 = 100$ in the presence of magnetic field $b_0 = 0.03$ (corresponding to $\sim 3 MG$ of magnetic field).

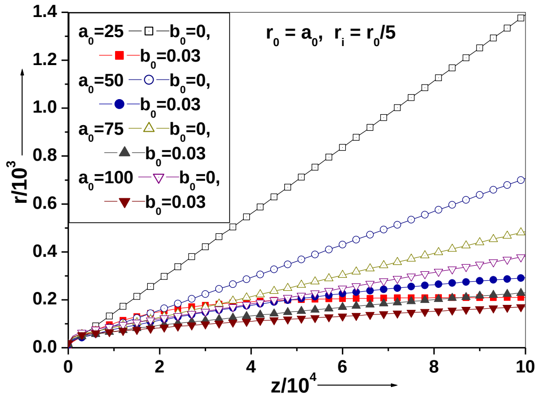

Figure 6.6 Trajectory of electron in the $r-z$ plane in the absence and presence of a magnetic field with $r_i = r_0/5$ and $r_0 = a_0$ for laser intensity parameters $a_0 = 25,\ 50,\ 75,$ and 100. Rest parameters are same as taken in fig. 6.4.

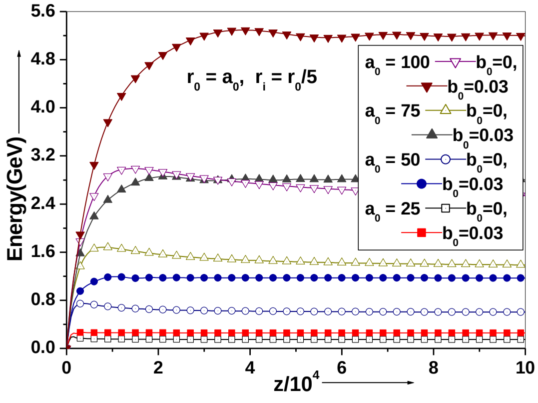

Figure 6.7. Electron energy gain with normalized distance in the absence and presence of a magnetic field with $r_i = r_0/5$ and $r_0 = a_0$ for laser intensity parameters $a_0 = 25,\ 50,\ 75,$ and 100. The other parameters are same as taken in fig. 6.4.

Yanovsky *et al.* [77] proposed that with a higher focal intensity laser pulse a tighter focal spot appears. We find $r_0 = a_0$ as an optimum value for higher energy gain with lowest scattering of accelerated electron. This is because of the longitudinal electric field of laser which is comparatively weaker with $r_0 > a_0$ than that with $r_0 \le a_0$. Whereas, with $r_0 < a_0$ the laser pulse diverges quickly, this reduces the duration of interaction of electron with laser pulse [97]. We have observed a relatively lower scattering of electrons in the presence of axial magnetic field with $r_i = r_0 / 5$ for $r_0 = a_0$ than that with $r_i = 0$ for $r_0 = a_0$ in the absence of axial magnetic field. Thus, axial magnetic field is supportive in keeping the accelerated electron in close to propagation axis.

6.5 CONCLUSION

Our model specifies the effect of an axial magnetic field on electron acceleration by a RP laser in vacuum. We have found that a high intensity RP laser pulse can accelerate a rest electron in the direction of propagation of laser pulse with small scattering. We have observed the relativistic electron acceleration to GeV energies in vacuum. The electron energy is further enhanced in the presence of axial magnetic field. The unique characteristics of RP beams with cylindrical symmetry in comparison with linearly or circularly polarized beams support better acceleration of small particles. The axial magnetic field enforces better trapping during interaction of electron with laser pulse. Thus a significant enhancement in electron energy gain with a relative smaller scattering appears. We have observed the sensitiveness of axial magnetic field on electron energy gain. A significant enhancement in electron energy gain with a relatively smaller scattering appears with axial magnetic field of small and optimum values. We have observed 70% enhancement in electron energy in the presence of axial magnetic field than in the absence of magnetic field.